METAL-MATRIX COMPOSITES

1. Introduction

A composite material (1) is a material consisting of two or more physically and/or chemically distinct phases. The composite generally has superior characteristics than those of each of the individual components. Usually, the reinforcing component is distributed in the continuous or matrix component. When the matrix is a metal, the composite is termed a metal-matrix composite (MMC). In MMCs, the reinforcement usually takes the form of particles, whiskers, short fibers, or continuous fibers (see COMPOSITE MATERIALS).

2. Types of Metal-Matrix Composites

Metal-matrix composites are generally distinguished by characteristics of the reinforcement: particle-reinforced MMCs, short fiber- or whisker-reinforced MMCs, and continuous fiber- or layered MMCs. Table 1 shows examples of some important reinforcements used in metal-matrix composites. These are categorized by the diameter and aspect ratio (length/diameter) of the reinforcement.

The aspect ratio of the reinforcement is an important quantity, because the degree of load transfer from the matrix to the reinforcement is directly proportional to the reinforcement aspect ratio. Thus, continuous fibers typically provide the highest degree of load transfer, because of their very high aspect ratio, which results in a significant amount of strengthening along the fiber direction. Particle or short fiber reinforced metals have a much lower aspect ratio, so they exhibit lower strengths than their continuous fiber counterparts, although the properties of these composites are much more isotropic. Figures 1**a** and **b** show typical microstructures of a continuous alumina fiber–Mg composite and silicon carbide particle–Al composite, respectively.

3. Processing

Metal-matrix composites can be processed by several techniques. Some of these important techniques are described below.

3.1. Liquid-State Processes. *Casting or Liquid Infiltration.* This process involves infiltration of a fibrous or particulate reinforcement preform by a liquid metal. Liquid-phase infiltration of MMCs is not straightforward, mainly because of difficulties with wetting the ceramic reinforcement by the molten metal. When the infiltration of a fiber preform occurs readily, reactions between the fiber and the molten metal may take place which significantly degrade the properties of the fiber. Fiber coatings (qv) applied prior to infiltration, which improve wetting and allow control of interfacial reactions, have been developed and are producing some encouraging results. In this case, however, the disadvantage is that the fiber coatings must not be exposed to air prior to infiltration

Table 1. **Typical Reinforcements Used in Metal-Matrix Composites**

Type	Aspect ratio	Diameter, μm	Examples
particle	~1–4	1–25	SiC, Al_2O_3, BN, B_4C
short fiber or whisker	~10–1000	0.1–25	SiC, Al_2O_3, $Al_2O_3 + SiO_2$, C
continuous fiber	>1000	3–150	SiC, Al_2O_3, C, B, W

because surface oxidation of the coating takes place (2). One liquid infiltration process involving particulate reinforcement, called the Duralcan process, has been quite successful (Fig. 2). Ceramic particles and ingot-grade aluminum are mixed and melted. The melt is stirred slightly above the liquidus temperature (600–700°C). The solidified ingot may also undergo secondary processing by extrusion or rolling. The Duralcan process of making particulate composites by a liquid metal casting route involves the use of 8–12-μm particles. For particles that are much smaller (2–3 μm), the result is a very large interface region and, thus, a very viscous melt. In foundry-grade MMCs, high Si aluminum alloys (eg, A-356) are used to prevent the formation of the brittle compound Al_4C_3, which is formed from the interfacial reaction between Al and SiC. The Al_4C_3 is extremely detrimental to mechanical properties, particularly toughness and corrosion resistance.

Alternatively, tows of fibers can be passed through a liquid metal bath, where the individual fibers are wet by the molten metal, wiped of excess metal, and a composite wire is produced. A bundle of such wires can be consolidated by extrusion to make a composite. Another pressureless liquid metal infiltration process of making MMCs is the Primex process (Lanxide), which can be used with certain reactive metal alloys such as Al–Mg to infiltrate ceramic preforms, Figure 3. For an Al–Mg alloy, the process takes place between 750–1000°C in a nitrogen-rich atmosphere, and typical infiltration rates are <25 cm/h.

Squeeze Casting or Pressure Infiltration. This process involves forcing a liquid metal into a fibrous or particulate preform (2–4) (Fig. 4). Pressure is applied until solidification is complete. By forcing the molten metal through small pores of the fibrous preform, this method obviates the requirement of good wettability of the reinforcement by the molten metal. Composites fabricated with this method have the advantage of minimal reaction between the reinforcement and molten metal because of the short processing time involved. Such composites are also typically free from common casting defects such

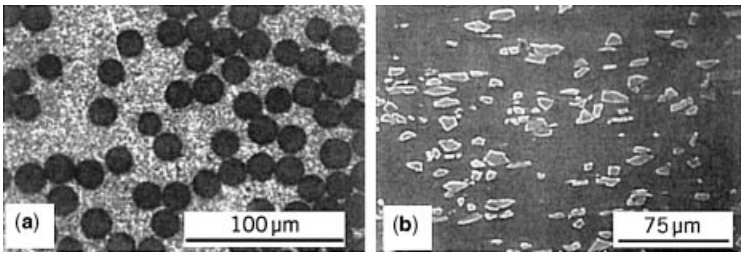

Fig. 1. Typical microstructures of some metal-matrix composites: (**a**) continuous alumina fiber–Mg composite and (**b**) silicon carbide particle–Al composite.

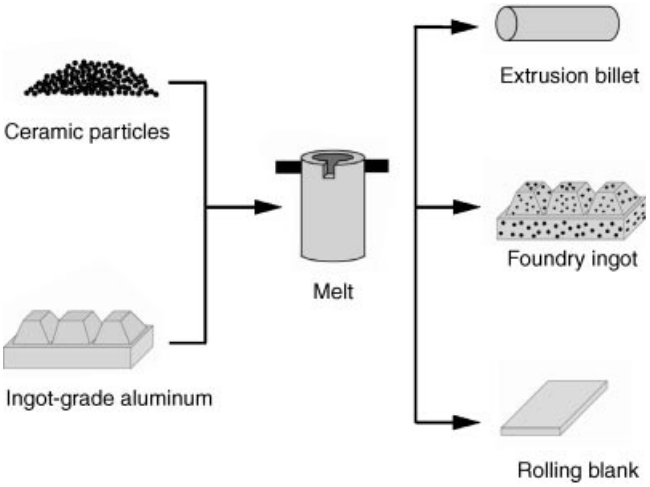

Fig. 2. Casting process for particulate or short fiber MMCs.

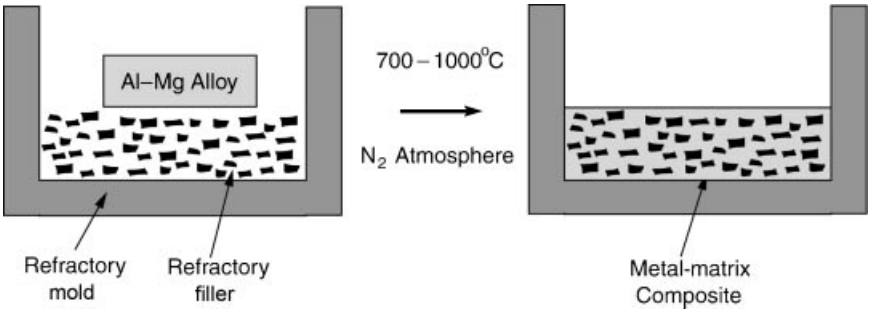

Fig. 3. Reactive liquid metal infiltration process.

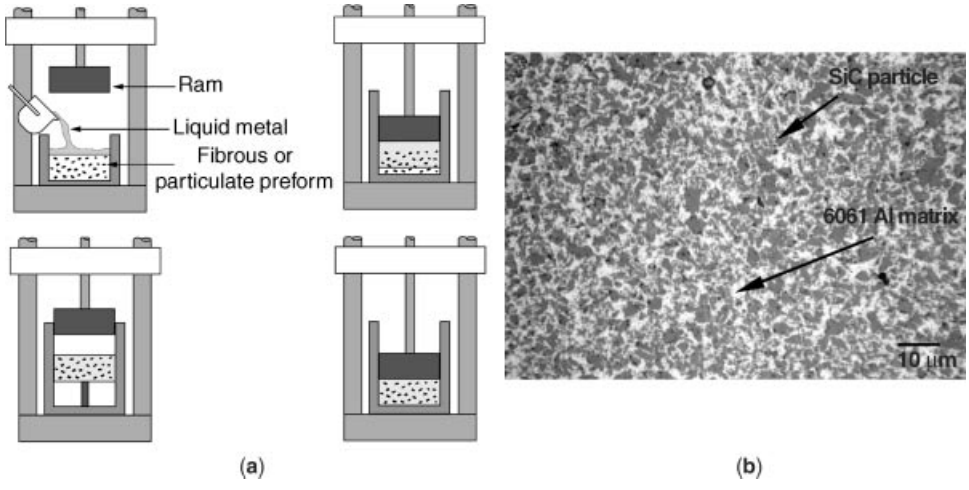

Fig. 4. (**a**) Squeeze casting or pressure infiltration process and (**b**) microstructure of 6061/SiC/50_p composite (from Ref. 4).

as porosity and shrinkage cavities. Infiltration of a fibrous preform by means of a pressurized inert gas is another variant of the liquid metal infiltration technique. The process is conducted in the controlled environment of a pressure vessel and rather high fiber volume fractions; complex shaped structures are obtainable (3,4). Alumina fiber-reinforced intermetallic matrix composites, eg, TiAl, Ni_3Al, and Fe_3Al matrix materials, have also been prepared by pressure casting (5). The technique involves melting of the matrix alloy in a crucible in vacuum, while the fibrous preform is heated separately. The molten matrix material (at $\sim$100°C above T_m) is poured onto the fibers and argon gas is introduced simultaneously. Argon gas-pressure forces the melt, which contains additives to aid wetting of the fibers, to infiltrate the preform.

3.2. Solid-State Processes. *Diffusion Bonding.* This process is a common solid-state processing technique for joining similar or dissimilar metals. Interdiffusion of atoms between clean metallic surfaces, in contact at an elevated temperature, leads to bonding. The principal advantages of this technique are the ability to process a wide variety of metal matrices and control of fiber orientation and volume fraction. Among the disadvantages are long processing times, high processing temperatures and pressures (which makes the process expensive), and a limitation on the complexity of shapes that can be produced. There are many variants of the basic diffusion bonding process, although all of them involve simultaneous application of pressure and high temperature. Matrix alloy foil and fiber arrays (composite wire) or monolayer laminae are stacked in a predetermined order (Fig. 5). Vacuum hot pressing is an important step in the diffusion bonding processes for metal-matrix composites. Hot isostatic pressing (HIP), instead of uniaxial pressing, can also be used. In HIP, gas pressure against a can consolidates the composite inside the can. With HIP it is relatively easy to apply high pressures at elevated temperatures with variable geometries.

Deformation Processing. This process can also be used to deform and/or densify the composite material. In metal–metal composites mechanical processing (swaging, extrusion, drawing, or rolling) of a ductile two-phase material causes the two phases to codeform, causing one of the phases to elongate and become fibrous in nature within the other phase. These materials are sometimes referred to as *in situ* composites. The properties of a deformation processed composite depend largely on the characteristics of the starting material, which is usually a billet of a two-phase alloy that has been prepared by casting or powder metallurgy methods (see METALLURGY, POWDER). Roll bonding is a common technique used to produce a laminated composite consisting of different metals in layered form (6). Such composites are called sheet laminated MMC. Roll bonding and hot pressing have also been used to make laminates of Al sheets and discontinuously reinforced MMCs (7,8). Figure 6 shows the roll bonding process for making a laminated MMC. Other examples of deformation processed MMC are niobium-based conventional filamentary superconductors with a copper matrix and the high T_C superconductors with a silver matrix. There are two main types of the conventional niobium-based superconductors: Nb-Ti/Cu and Nb_3Sn/Cu. Niobium–titanium ($\sim$50–50) form a ductile system. Rods of Nb-Ti are inserted in holes drilled in a block of copper, evacuated, sealed, and subjected to a series of drawing operations interspersed with appropriate annealing

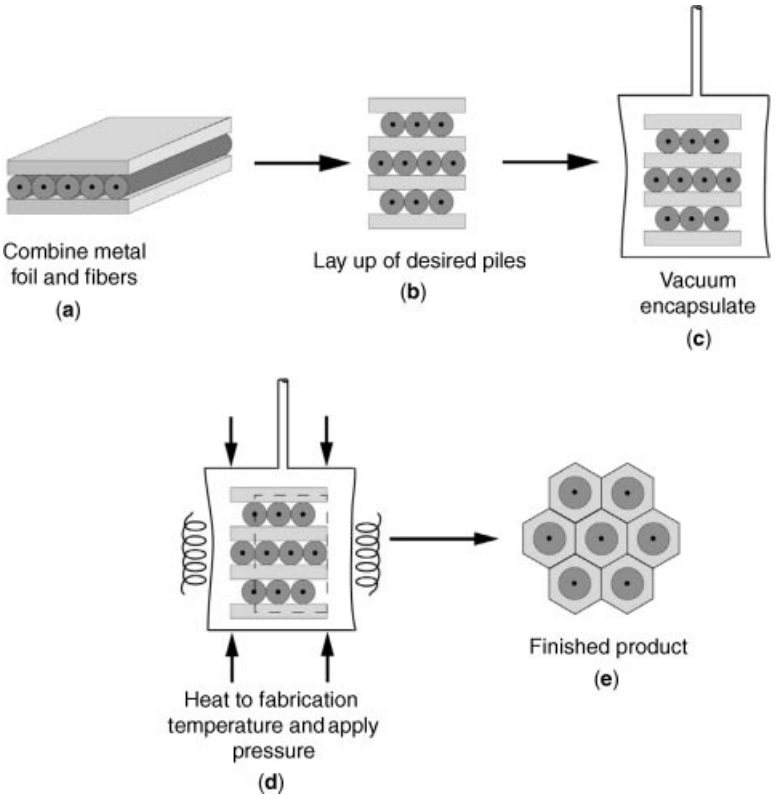

Fig. 5. Diffusion bonding process: (**a**) apply metal foil and cut to shape, (**b**) lay up desired plies, (**c**) vacuum encapsulate and heat to fabrication temperature, (**d**) apply pressure and hold for consolidation cycle, and (**e**) cool, remove, and clean part.

treatments to obtain the final composite superconducting wire. In the case of Nb_3Sn/Cu, a process called the bronze route is used to make this composite. Nb_3Sn, an A-15-type intermetallic, cannot be processed like Nb-Ti because of its extreme brittleness. Instead, the process starts with a bronze (Cu–13% Sn) matrix; pure niobium rods are inserted in holes drilled in bronze, evacuated, sealed, and subjected to wire drawing operations as in the case of Nb-Ti/Cu.

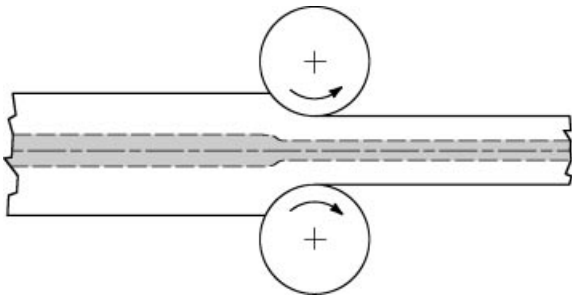

Fig. 6. Roll bonding process of making a laminated MMC; a metallurgical bond is produced.

The critical step is the final heat treatment (~700°C) that drives out the tin from the bronze matrix to combine with niobium to form stoichiometric, superconducting Nb_3Sn, leaving behind copper matrix. A similar process, called the oxide-powder-in-tube (OPIT) method (9), is used to fabricate silver matrix high T_C superconducting composites. In this process, the oxide powder of appropriate composition (stoichiometry, phase content, purity, etc) is packed inside a metal tube (generally silver), sealed, and degassed. Commonly, swaging and drawing are used to make wires and rolling is used for tapes. Heat treatments, intermediate and/or subsequent to deformation, are conducted to form the desired phase, promote grain interconnectivity and crystallographic alignment of the oxide, and obtain proper oxygenation (9).

Powder Processing. In conjunction with deformation processing these methods are used to fabricate particulate or short fiber reinforced composites. This typically involves cold pressing and sintering, or hot pressing to fabricate primarily particle- or whisker-reinforced MMCs (10). The matrix and the reinforcement powders are blended to produce a homogeneous distribution, Figure 7. The blending stage is followed by cold pressing to produce what is called a green body, which is ~80% dense and can be easily handled. The cold pressed green body is canned in a sealed container and degassed to remove any absorbed moisture from the particle surfaces. The material is hot pressed, uniaxially or isostatically, to produce a fully dense composite and extruded. The rigid particles or fibers cause the matrix to be deformed significantly. In addition, during hot extrusion, dynamic recrystallization takes place at the particle–matrix interface, yielding randomly oriented grains near the interface, and relatively textured grains far from the interface, Figure 8 (11).

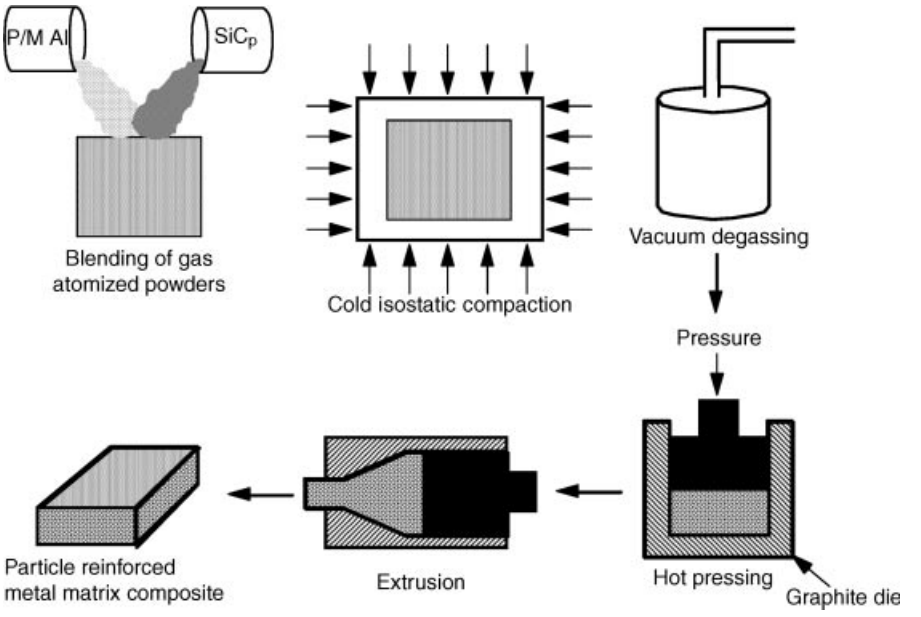

Fig. 7. Powder processing, hot pressing, and extrusion process for fabricating particulate or short fiber reinforced MMCs.

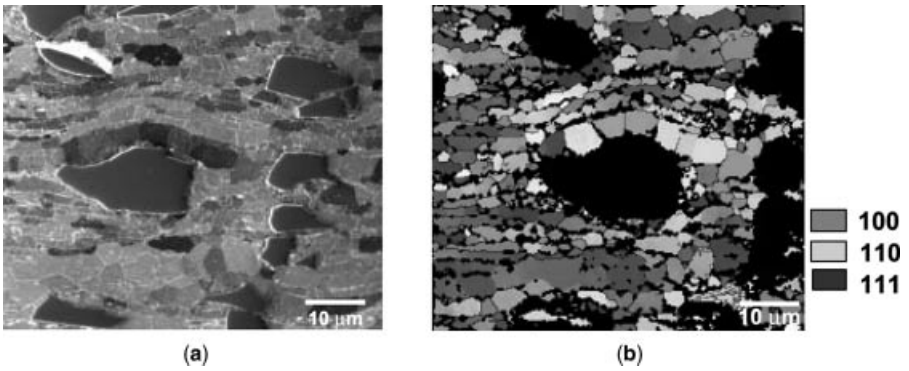

Fig. 8. (**a**) Microstructure of SiC particle reinforced 2080 Al matrix composite after hot extrusion and (**b**) Orientation image map showing random orientation of grains at the particle/matrix interface due to dynamic recrystallization, and textured grains away from the interface (from Ref. 11).

Sinter Forging. This process is a novel and low cost deformation processing technique (12). In sinter-forging a powder mixture of reinforcement and matrix is cold compacted, sintered, and forged to nearly full density, Figure 9. The main advantage of this technique is that forging is conducted to produce a near-net shape material, and machining operations and material waste are minimized. The low cost, sinter-forged composites have tensile and fatigue properties that are comparable to those of materials produced by extrusion.

Deposition Techniques. This process for MMC fabrication involves coating individual fibers in a tow with the matrix material needed to form the composite followed by diffusion bonding to form a consolidated composite plate or structural shape. The main disadvantage of using deposition techniques is that they are time consuming. However, there are several advantages. (*1*) The degree of interfacial bonding is easily controllable; interfacial diffusion barriers and compliant coatings can be formed on the fiber prior to matrix deposition or

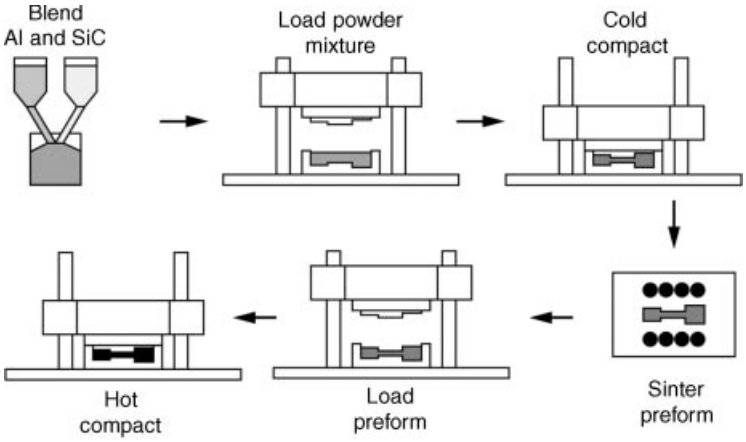

Fig. 9. Sinter-forging technique for producing near-net shape, low cost MMCs (from Ref. 12).

graded interfaces can be formed. (*2*) Filament-wound thin monolayer tapes can be produced that are easier to handle and easier to mold into structural shapes than other precursor forms; unidirectional or angle-plied composites can be easily fabricated in this way.

Several deposition techniques are available: immersion plating, electroplating, spray deposition, chemical vapor deposition (CVD), and physical vapor deposition (PVD) (see THIN FILMS). Dipping or immersion plating is similar to infiltration casting except that fiber tows are continuously passed through baths of molten metal, slurry, sol, or organometallic precursors. Electroplating (qv) produces a coating from a solution containing the ion of the desired material in the presence of an electric current. Fibers are wound on a mandrel, which serves as the cathode, and placed into the plating bath with an anode of the desired matrix material. The advantage of this method is that the temperatures involved are moderate and no damage is done to the fibers. Problems with electroplating involve void formation between fibers and between fiber layers, possible poor adhesion of the deposit to the fibers, and limited numbers of alloy matrices available for this type of processing. A spray deposition operation may also be used. This technique typically consists of winding fibers onto a foil-coated drum and spraying molten metal onto them to form a monotape. The source of molten metal may be powder or wire feedstock which is melted in a flame, arc, or plasma torch. The advantages of spray deposition are the easier control of fiber alignment and rapid solidification of the molten matrix. In the CVD process, a vaporized component decomposes or reacts with another vaporized chemical on the substrate to form a coating on that substrate. The processing is generally carried out at elevated temperatures.

PVD may also be used to produce multilayered MMCs, particularly at the nanometer scale. An example of such a multilayered MMC microsturcture with individual layers on the nanometer scale is shown in Figure 10 (13). Figure 10(**a**) shows the microstructure of a multilayered Al/SiC composite with progressively thicker layers. Figure 10(**b**) shows a comparison of the tensile behavior of a multilayered composite (with layers of uniform thickness) with that of a single Al film. The total layer was 500 nm in thickness, with individual SiC layers ~25 nm and Al layers ~105 nm. Note that the composite had a significantly higher strength than a pure Al film of similar thickness.

3.3. *In Situ* Processes. In these techniques, the reinforcement phase is formed *in situ*. The composite material is produced in one step from an appropriate starting alloy, thus avoiding the difficulties inherent in combining the separate components as done in a typical composite processing. Controlled unidirectional solidification of a eutectic alloy is a classic example of *in situ* processing, Figure 11. Unidirectional solidification of a eutectic alloy typically results in one phase being distributed in the form of fibers or ribbon in the matrix phase. The relative size and spacing of the reinforcement phase can be controlled by simply controlling the solidification rate, although the volume fraction of reinforcement will always be constant. The solidification rate in practice, however, is limited to a range of 1–5 cm/h because of the need to maintain a stable growth front which requires a high temperature gradient.

The XD process (patented by Martin Marietta) is another *in situ* process that uses an exothermic reaction between two components to produce a third

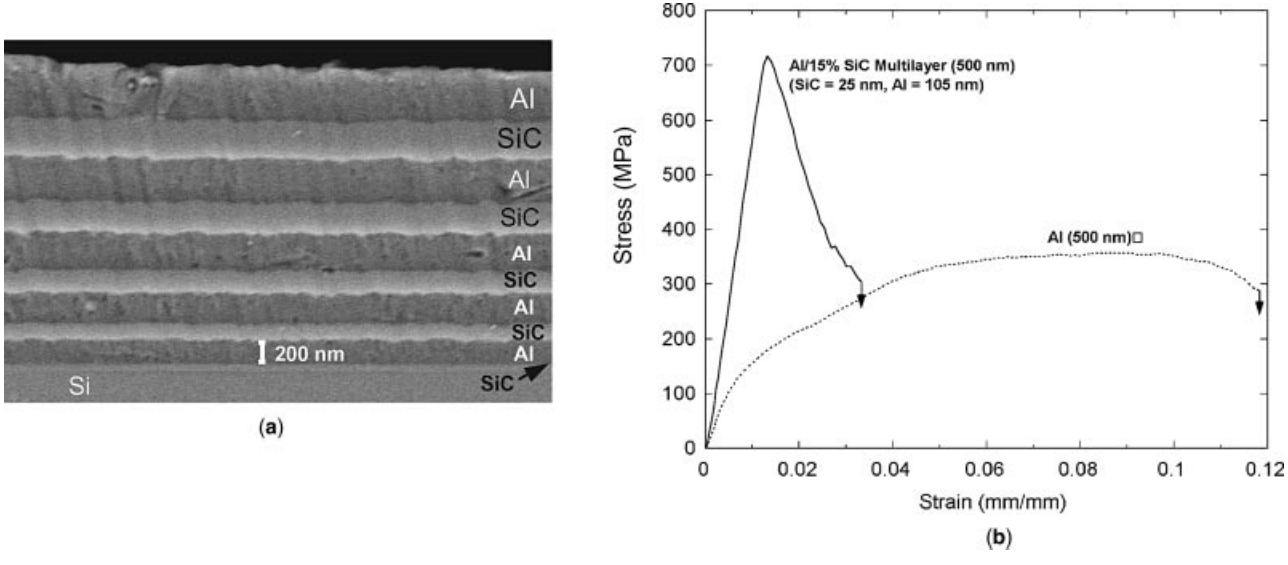

Fig. 10. (**a**) Microstructure of multilayered Al/SiC composite deposited by PVD. The thickness of the layers increases progressively with distance from the Si substrate. (**b**) Comparison of tensile behavior between Al/SiC multilyer (500 nm, with homogeneous individual layer thickness) compared to Al film. Note the significantly higher strength in the multilayer MMC (from Ref. 13).

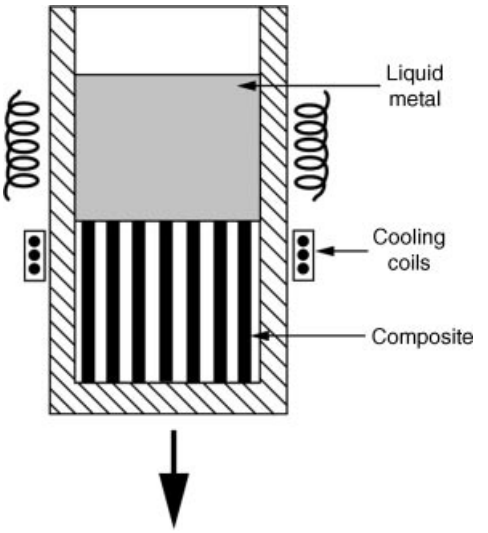

Fig. 11. *In situ* processing by controlled unidirectional solidification of a eutectic alloy.

component. Sometimes such processing techniques are referred to as self-propagating high temperature synthesis (SHS) process. Specifically, the XD process is a proprietary process developed to produce ceramic particle-reinforced metallic alloy. Generally, a master alloy containing a high volume fraction of reinforcement is produced by the reaction synthesis. This is mixed and remelted with the base alloy to produce the desirable amount of particle reinforcement. Typical reinforcements used include SiC or TiB_2 in an aluminum, nickel, or an intermetallic matrix.

3.4. Spray-Forming of Particulate MMCs. Another process for making particle-reinforced MMCs involves the use of modfied spray forming techniques that have been used to produce monolithic alloys for some time (14). One particular example of this, a co-spray process, uses a spray gun to atomize a molten aluminum alloy matrix, into which heated silicon carbide particles are injected (Fig. 12). An optimum particle size is required for efficient transfer, eg, whiskers are too fine to be transferred. The preform produced is generally quite porous. The cosprayed MMC is subjected to scalping, consolidation, and secondary finishing processes to form a wrought composite. The spray process is generally automated and quite fast, but it should be noted that it is essentially a liquid metallurgy process. The formation of deleterious reaction products is generally avoided because the time of flight of the composite particles is extremely short. Silicon carbide particles of an aspect ratio (length/diameter) between 3–4 and volume fractions up to 20% have been incorporated into aluminum alloys. An advantage of the process is the flexibility it provides in making different types of composites, eg, *in situ* laminates can be made using two sprayers or by selective reinforcement. This process is quite expensive, however, mainly because of the costly capital equipment.

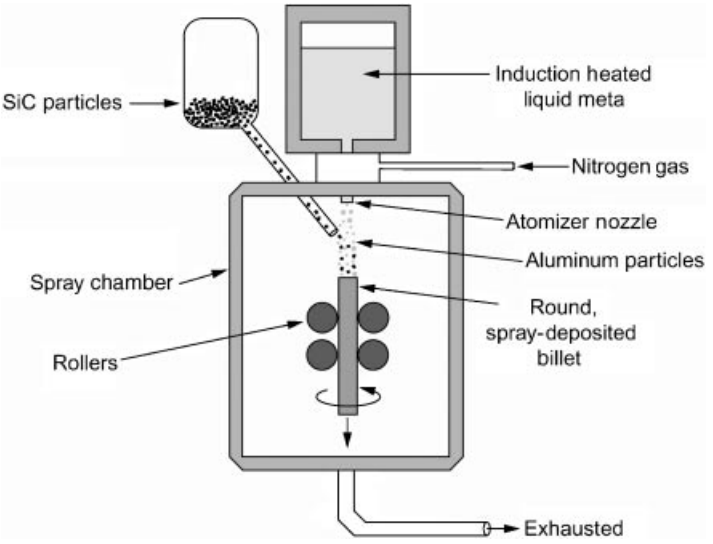

Fig. 12. The spray-forming process.

4. Interfaces in Metal-Matrix Composites

The interface region in a composite is extremely important in determining the ultimate properties of the composite. At the interface, a discontinuity occurs in one or more material parameters such as elastic modulus, thermodynamic parameters such as chemical potential, and coefficient of thermal expansion. The importance of the interface region in composites stems from two main factors: The interface occupies a large area in composites, and in general, the reinforcement and the matrix form a system that is not in thermodynamic equilibrium.

In crystallographic terms, ceramic–metal interfaces in composites generally are incoherent, high energy interfaces. Accordingly, they can act as efficient vacancy sinks, and provide rapid diffusion paths, segregation sites, and sites for heterogeneous precipitation, as well as sites for precipitate-free zones (eg, in an age-hardenable matrix). Among the possible exceptions to this are the eutectic composites (1) and the XD-type particulate composites (15).

Some degree of bonding must exist between the ceramic reinforcement and the metal matrix to enable load transfer from matrix to fiber. Two main categories of bonding are mechanical and chemical. Mechanical keying effects between two surfaces can lead to bonding. This has been confirmed experimentally for tungsten filaments in an aluminum matrix (16). Mechanical gripping effects have also been observed at interfaces between Al_2O_3 and Al (17); these results are shown in the form of crack density in alumina as a function of strain in the alumina–aluminum composite for different degrees of interface roughness, Figure 13. The crack density continues to increase to larger strain values in the case of a rough interface while it reaches a plateau value for the smooth or slightly rough Interface. Most MMC systems, however, are nonequilibrium systems in the thermodynamic sense; that is, there exists a chemical

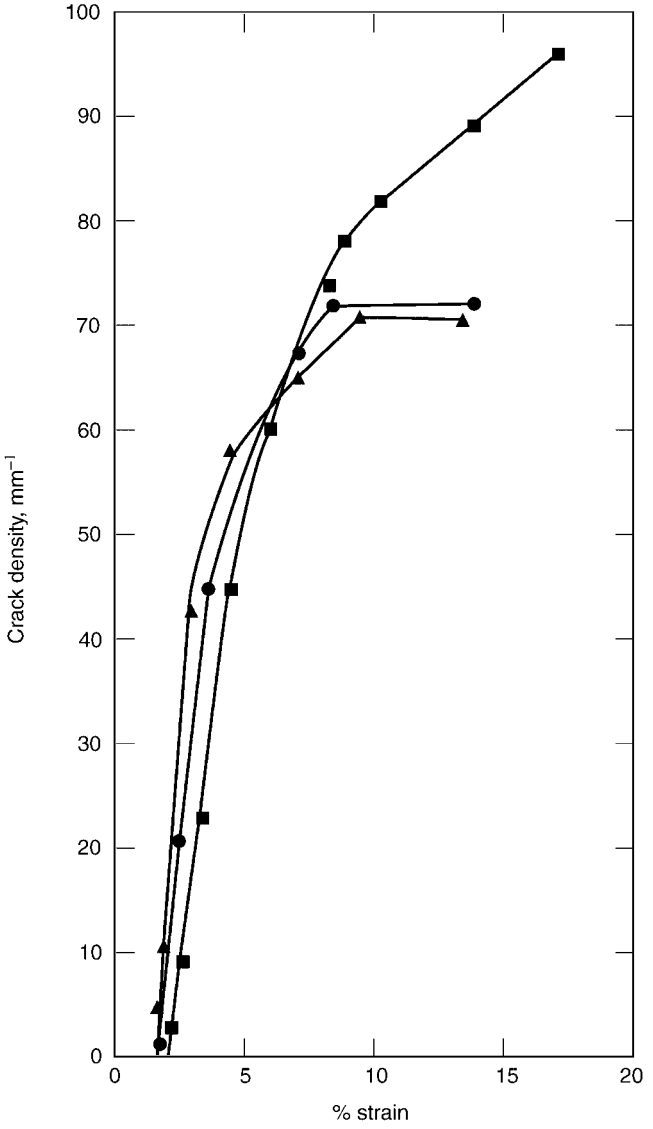

Fig. 13. Number of cracks per mm vs percent strain in an alumina/aluminum composite for different degrees of roughness where (•) represents the polished substrate or smooth interface; (■), steep sided pits, $10^6/cm^2$ or rough interface; and (▲), gently sloping pits, $10^3/cm^2$ or smooth roughness. The crack density continues to increase to larger strain values in the case of a rough interface while it reaches a plateau value for the smooth or slightly rough interface (from Ref. 16).

potential gradient across the fiber/matrix interface. This means that given favorable kinetic conditions, which in practice means a high enough temperature or long enough time, diffusion and/or chemical reactions occur between the components. Figure 14 shows a dark field (DF) transmission electron microscopy (TEM) micrograph showing a reaction zone (RZ) between alumina fiber and magnesium matrix. The lenticular shaped regions are deformation twins in the Mg

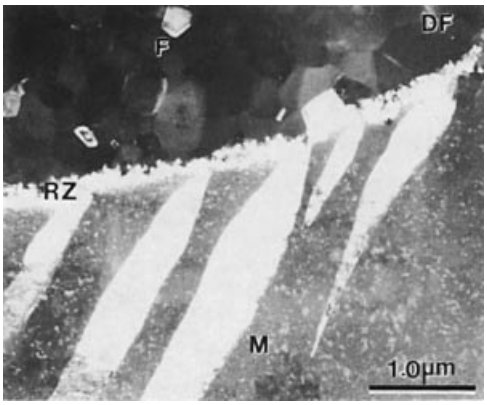

Fig. 14. A dark field (DF) transmission electron micrograph showing interface in a continuous fiber (F) α-Al_2O_3 (F)/Mg alloy (ZE41A) matrix (M) within the reaction zone (RZ). The lenticular shaped regions are deformation twins in the Mg alloy matrix that resulted because of palstic deformation during cool down from the processing temperature.

alloy matrix that resulted because of plastic deformation during cool down from the processing temperature to room temperature. Note that at times some controlled amount of reaction at the interface (Fig. 14) may be desirable for obtaining strong bonding between the fiber and the matrix; however, too thick an interaction zone adversely affects the mechanical properties of the composite.

Finally, ceramic–metal interfaces are generally formed at high temperatures. Diffusion and chemical reaction kinetics are faster at elevated temperatures. Knowledge of the chemical reaction products and, if possible, their properties are needed. It is therefore imperative to understand the thermodynamics and kinetics of reactions such that processing can be controlled and optimum properties obtained.

5. Properties

5.1. Young's Modulus. Unidirectionally reinforced continuous fiber-reinforced MMCs show a linear increase in the longitudinal Young's modulus as a function of fiber volume fraction. Figure 15 shows an example of modulus increase as a function of fiber volume fraction for an alumina fiber-reinforced aluminum–lithium alloy matrix composite (18). The increase in the longitudinal Young's modulus is in agreement with the rule-of-mixtures value, whereas the modulus increase in a direction transverse to the fibers is much lower. Particle reinforcement also results in an increase in the modulus of the composite; the increase, however, is much less than that predicted by the rule-of-mixtures. This is understandable inasmuch as the rule of mixtures is valid only for continuous fiber reinforcement. Figure 16 shows increase in Young's modulus in an aluminum composite with volume fraction of silicon carbide particles (19). Note that due to particle orientation along the extrusion axis, the modulus along the longitudinal orientation (parallel to the extrusion axis) is higher than perpendicular to extrusion

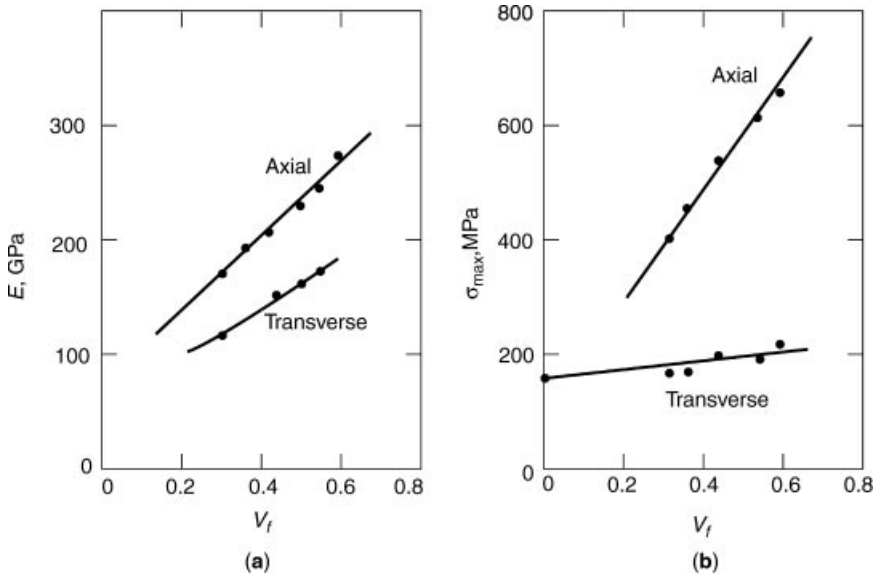

Fig. 15. Modulus increase as a function of fiber volume fraction V_f for alumina fiber-reinforced aluminum–lithium alloy matrix for (**a**) E (elastic modulus), and (**b**) σ_{max} (from Ref. 18). To convert MPa to psi, multiply by 145.

(transverse orientation). Thus, there is a loss of reinforcement efficiency in going from continuous fiber to particle. Metal-matrix particulate composites such as SiC particle-reinforced aluminum can offer a 50–100% increase in modulus over that of unreinforced aluminum, ie, the modulus equivalent to that of titanium but density that is ~33% lower. Also, unlike fiber-reinforced composites, the stiffness enhancement in particulate composites is reasonably isotropic.

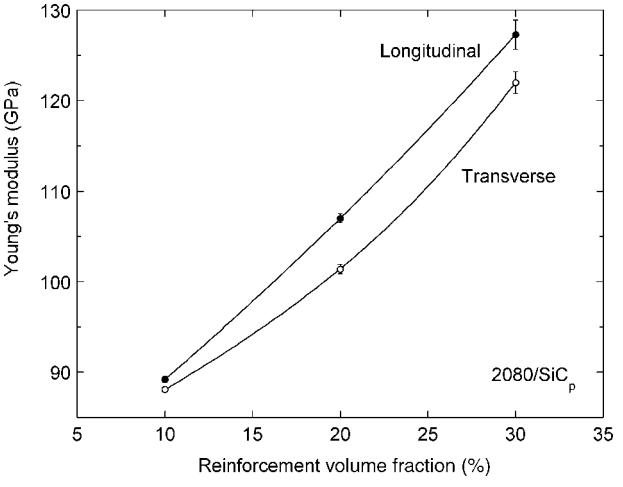

Fig. 16. Young's modulus increase in an aluminum composite with SiC particle reinforcement volume fraction (from Ref. 19). To convert GPa to psi, multiply by 145,000.

5.2. Strength. Prediction of MMC strength is more complicated than the prediction of elastic modulus. Consider an aligned fiber-reinforced MMC under a load P_c in the direction of the fibers. This load is distributed between the fiber and the matrix:

$$P_c = P_m V_m + P_f V_f$$

where P_m and P_f are loads on the matrix and fiber, respectively. This equation can be converted to the following rule-of-mixtures relationship under conditions of isostrain, ie, the strain in the fiber, matrix, and composite are equal:

$$\sigma_c = \sigma_f V_f + \sigma_m V_m$$

where σ is the stress, V is the volume fraction, and c, f, and m denote composite, fiber, and matrix, respectively. This rule-of-mixtures equation says that the strength of the composite is a volume weighted average of the strengths of the fiber and matrix. This is correct provided the *in situ* values of the strength of fiber and matrix are used. If the fiber remains essentially elastic up to the point of fracture, the fiber strength in the composite, σ_f, is the same as that determined in a test of the fiber individually. This is particularly true of ceramic fibers. However, the same cannot be said for the metallic matrix. The matrix strength in the composite (*in situ* strength) is not the same as that determined from a test of an unreinforced matrix sample in isolation because the metal matrix can suffer several microstructural changes during processing, and consequently changes in its mechanical properties. In view of the fact that, in general, ceramic reinforcements have a coefficient of thermal expansion smaller than that of most metallic matrices, thermal stresses are generated in both the components, the fiber and the matrix. The reinforcement also acts as a constraint on the matrix flow, thus increasing its flow stress. A series of events can take place in response to the thermal stresses (20–23): (*1*) plastic deformation of the ductile metal matrix (slip, twinning, cavitation, grain boundary sliding, and/or migration); (*2*) cracking and failure of the brittle fiber; (*3*) an adverse reaction at the interface; and (*4*) failure of the fiber–matrix interface. These changes can result in the *in situ* of the matrix to be different from that of the matrix material in isolation.

The strength *in situ* MMC is given by a relationship similar to the Hall-Petch relationship used for grain boundary strengthening of metals:

$$\sigma = \sigma_0 + k\lambda^{-1/2}$$

where σ_0 is a friction stress term, k is a material constant, and λ is the spacing between rods or lamellae (24). The interfiber spacing, λ, can be varied rather easily by controlling the solidification rate, R, because $\lambda^2 \mathrm{R} = \text{constant}$.

5.3. Toughness. Toughness can be regarded as a measure of energy absorbed in the process of fracture or more specifically as the resistance to crack propagation, K_{Ic}. The toughness of MMCs depends on matrix alloy composition and microstructure; reinforcement type, size, and orientation; and processing insofar as it affects microstructural variables, eg, distribution of reinforcement, porosity, segregation, etc.

Table 2. **Impact Fracture Energy of B/Al 1100**[a]

Fiber diameter, μm	Energy,[b] kJ/m^2
100	90
140	150
200	200–300

[a] Ref. 22.
[b] To convert kJ/m^2 to $ft \cdot lbf/in^2$, divide by 2.10.

For a given V_f, the larger the diameter of the fiber, the tougher the composite. This is because the larger the fiber diameter for a given fiber volume fraction, the larger the amount of tough, metallic matrix in the interfiber region that can undergo plastic deformation and thus contribute to the toughness. Table 2 shows this effect of fiber diameter on the impact fracture energy for a boron fiber–aluminum composite system (25).

Unidirectional fiber reinforcement can lead to easy crack initiation and propagation compared to the unreinforced alloy matrix. Braiding of fibers can make the crack propagation toughness increase tremendously because of extensive matrix deformation, fiber bundle debonding, and pullout. Table 3 summarizes this effect of fiber braiding (26). The fracture energy is the maximum for a composite consisting of three-dimensionally (30) arranged alumina fibers in an aluminum matrix.

The general range of K_{Ic} values for particle-reinforced aluminum-type MMCs is between 15 and 30 $MPa \cdot m^{1/2}$, whereas short fiber- or whisker-reinforced MMCs have >5–10 $MPa \cdot m^{1/2}$. Table 4 gives fracture toughness data for silicon carbide whisker (SiC_w) and silicon carbide particle (SiC_p) reinforced aluminum composites (27).

5.4. Thermal Stresses. In general, ceramic reinforcements (fibers, whiskers, or particles) have a coefficient of thermal expansion lower than that of most metallic matrices. This means that when the composite is subjected to a temperature change, thermal stresses are generated in both components. Figure 17 shows a microstructure-based simulation of thermal stresses in an SiC particle reinforced Al matrix composite (28). Note that thermal residual stresses develop in the SiC and Al, and they are exacerbated in regions of particle clustering.

Table 3. **Effect of Fiber Braiding on Fracture Energy of Alumina Fiber–Al–Li Composite**[a]

Material	Initiation energy, J[b]	Propagation energy, J[b]	Total fracture energy, J[b]
Al-2.5 Li alloy	173	145	218
0.34 V_f alumina/Al-Li unidirectional	62	79	141
0.36 V_f alumina/Al-Li 3D braided	68	196	264

[a] Ref. 23.
[b] To convert J to $ft \cdot lb$, divide by 1.356.

Table 4. **Toughness of SiC Particle and Whisker Reinforced 6061 Al**[a]

Material	K_{Ic},MPa · m$^{1/2}$
20 v/o SiC_w/6061-T6 Al	7.1
25 v/o SiC_p/6061-T6 Al	15.8
6061-T6Al	37.0

[a] Ref. 24.

Work involving a single-crystal copper matrix containing large diameter tungsten fibers has unequivocally shown the importance of thermal stresses in MMCs (20). A dislocation etch-pitting technique was employed to delineate dislocations in a single-crystal copper matrix and it was shown that near the fiber the dislocation density was much higher in the matrix than the dislocation density far away from the fiber. The situation in the as-cast composite can be depicted as there being a hard zone (high dislocation density) around each fiber and a soft zone (low dislocation density) away from the fiber. The enhanced dislocation density in the copper matrix near the fiber arises because of the plastic deformation in response to the thermal stresses generated by the thermal mismatch between the fiber and the matrix. The intensity of the gradient in dislocation density depends on the interfiber spacing. The dislocation density gradient decreases with a decrease in the interfiber spacing. The existence of a plastically deformed zone containing a high dislocation density in the metallic matrix in the vicinity of the reinforcement has been confirmed by transmission electron microscopy, both in fibrous and particulate MMCs (29). An example of dislocations generated near the interface is shown in Figure 18.

Thermal expansion mismatch between the reinforcement and the matrix is an important consideration. It should also be recognized that it is something that is difficult to avoid in any composite, however, the overall thermal expansion characteristics of a composite can be controlled by controlling the proportion of reinforcement and matrix and the distribution of the reinforcement in the

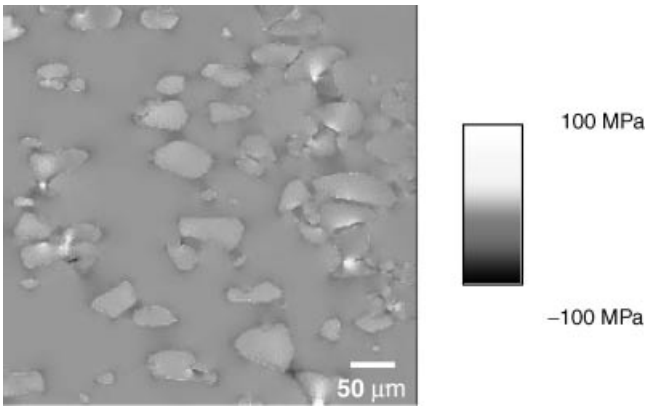

Fig. 17. Microstructure-based simulation of thermal residual stresses in a SiC particle reinforced Al matrix composite (from Ref. 28).

Fig. 18. Transmission electron micrograph (TEM) showing dislocations in aluminum in the region near a silicon carbide particle, SiC_p.

matrix. Many models have been proposed to predict the coefficients of thermal expansion of composites, and analyze the general thermal expansion characteristics of MMCs (30–33). Some experimental measurements and theoretical and numerical model predictions of thermal expansion behavior of a particulate MMC are shown in Figure 19 (28).

5.5. Aging. Frequently, the metal-matrix alloy used in an MMC has precipitation hardening characteristics, ie, such an alloy can be hardened by suitable heat treatment called aging. It has been shown that the microstructure of the metallic matrix is modified by the presence of ceramic reinforcement. In particular, a higher dislocation density in the matrix metal or alloy than that in the unreinforced metal or alloy is produced. The higher dislocation density in the matrix has its origin in the thermal mismatch, $\Delta\alpha$, between the reinforcement

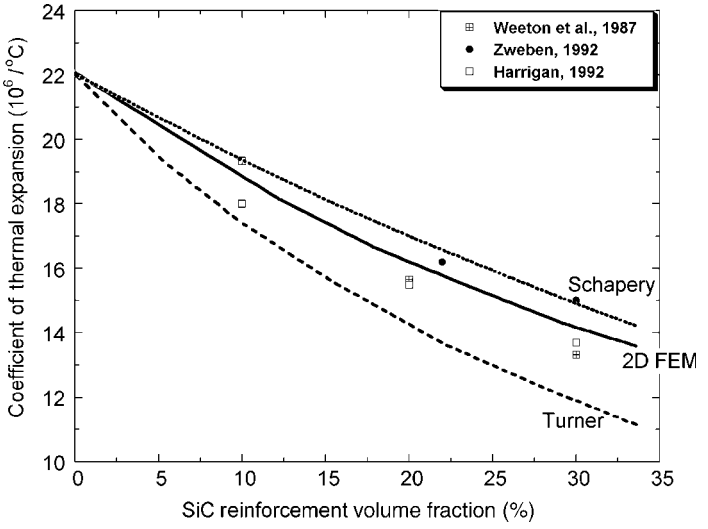

Fig. 19. Experimental measurements and theoretical and numerical model predictions of thermal expansion behavior of a particulate MMC (from Ref. 28).

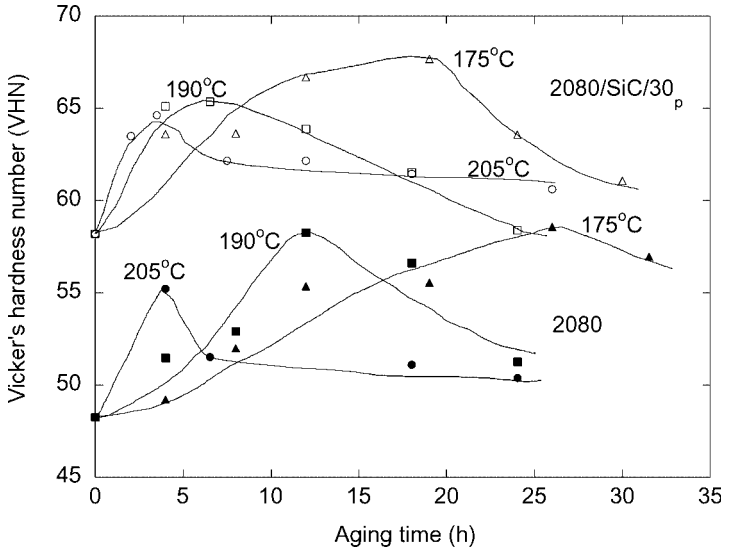

Fig. 20. Aging behavior of a particle reinforced MMC versus the unreiforced matrix alloy. Note the acceleration in aging of the composite due to enhanced precipitation at dislocations at the particle–matrix interface.

and the metallic matrix. This thermal mismatch can be quite large, eg, in the case of SiC and aluminum it has a high value of 21×10^{-6}/K. The high dislocation density enhances the precipitation kinetics in a precipitation hardenable matrix, such as 2XXX series aluminum alloy due to heterogeneous nucleation of precipitates at dislocations in the matrix of the composite. A considerable strength increment results due to age hardening treatments. More importantly, for a given temperature, an acceleration in aging takes place, Figure 20. Thus, a standard aging treatment for, eg, an unreinforced aluminum alloy, is not likely to be valid for the composite (34–37). This has important practical implications, ie, one may not use the standard heat treatments commonly available in various handbooks, eg, for monolithic aluminum alloys for an alloy used as a matrix in an MMC.

5.6. Fatigue. This phenomenon of mechanical property degradation leads to failure of a material or a component under cyclic loading. Many high volume applications of composite materials involve cycling loading situations, eg, automobile components. Application of conventional approaches, such as the stress vs cycle (S–N) curves or the application of linear elastic fracture mechanics (LEFM) to fatigue of composites, is not straightforward. The main reasons for this are the inherent heterogeneity and anisotropic nature of the composites which result in damage mechanisms in composites being very different from those encountered in conventional, homogeneous, or monolithic material. Novel approaches, such as measurement of stiffness reduction as a function of cycles, are being used to analyze the fatigue behavior of MMCs. Because many applications of composite MMCs involve temperature changes, it is important that thermal fatigue characteristics of composites be evaluated in addition to their mechanical fatigue characteristics.

Fatigue Crack Initiation. Processing-related defects in the form of intermetallic inclusions or particle clusters play an important role as fatigue crack initiating sites, particularly in powder metallurgy processed materials (38,39). These defects act as stress concentrators that increase the local stress intensity in the material and promote easy crack nucleation. Several researchers have shown that crack initiation during fatigue takes place at these defects, which are typically located at the surface of the specimen (38,40). The reason is that inclusions at the surface are more highly stressed than inclusions completely within the matrix (where more load is borne by the reinforcement), so a higher stress concentration and, thus, higher probability for crack initiation is present at the surface. For a given inclusion size, the stress concentration in a composite where the inclusion is surrounded by high stiffness reinforcement particles, is lower than in the unreinforced alloy. Since more of the load is being carried by the high stiffness SiC particles in the composite, an inclusion in the composite will be subjected to lower stress than a similar inclusion in the unreinforced alloy. In extruded materials, the overall size of inclusions is also lower in composites since the ceramic reinforcement particles break the brittle inclusions into smaller sizes during extrusion.

S–N Curves. A rule-of-thumb approach in fatigue of monolithic metals is to increase their monotonic strength that concomitantly results in an increase in cyclic strength. This rule assumes that the ratio of fatigue strength to tensile strength is about constant. It is generally true that the maximum efficiency in terms of stiffness and strength gains in fiber-reinforced composites occurs when the fibers are continuous, uniaxially aligned, and the properties are measured parallel to the fiber direction. Going off-angle, the role of the matrix becomes more important. Because of the highly anisotropic nature of the fiber-reinforced composites in general, the fatigue strength of off-axis MMCs (just like that of any other kind of off-axis fibrous composite), decreases with increasing angle between the fiber axis and the stress axis. In a study of the fatigue behavior of tungsten fiber-reinforced aluminum–4% copper alloy under tension compression cycling it was found that increasing the fiber volume fraction from 0 to 24% resulted in increased fatigue resistance (41). This was a direct result of increased monotonic strength of the composite as a function of the fiber volume fraction.

In terms of general S–N curve behavior, a composite such as a silicon carbide particle-reinforced aluminum alloy shows an improved fatigue behavior compared to the reinforced alloy, Figure 21 (8,39,42). Such an improvement in stress controlled cyclic loading or high cyclic fatigue is attributed to the higher stiffness of the composite. However, the fatigue behavior of the composite, evaluated in terms of strain amplitude vs cycles or low cycle fatigue, was found to be inferior to that of the unreinforced alloy (43). This was attributed to the lower ductility of the composite compared to the unreinforced alloy. At elevated temperatures, particularly close to the aging temperature for age hardenable alloys, the matrix strength decreases resulting in a decrease in fatigue strength, Figure 22 (44).

Fatigue Crack Propagation Tests. One significant drawback of studies on fatigue behavior of a material using this S–N approach is that no distinction can be made between the crack initiation phase and the crack propagation phase.

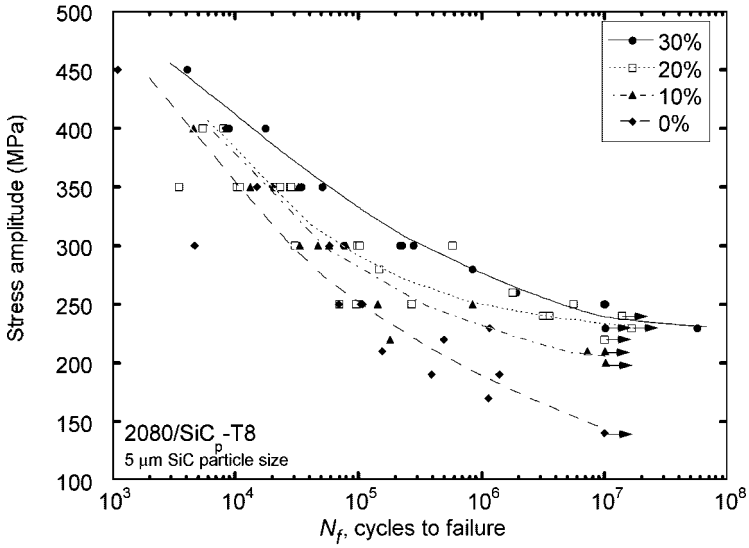

Fig. 21. Stress vs cycles (S–N) behavior of a particle reinforced MMC. With increasing volume fraction of particles the fatigue strength of the composite increases (from Ref. 42).

Tests on notched or precracked samples, generally conducted in an servohydraulic closed-loop testing machine, provide results in the form of crack growth per cycle, $\log(da/dN)$ vs cyclic stress intensity factor $\log \Delta K$. Crack growth rate, da/dN, is related to the cyclic stress intensity factor range, ΔK, according to the power law relationship first formulated in 1963, where A and m depend on

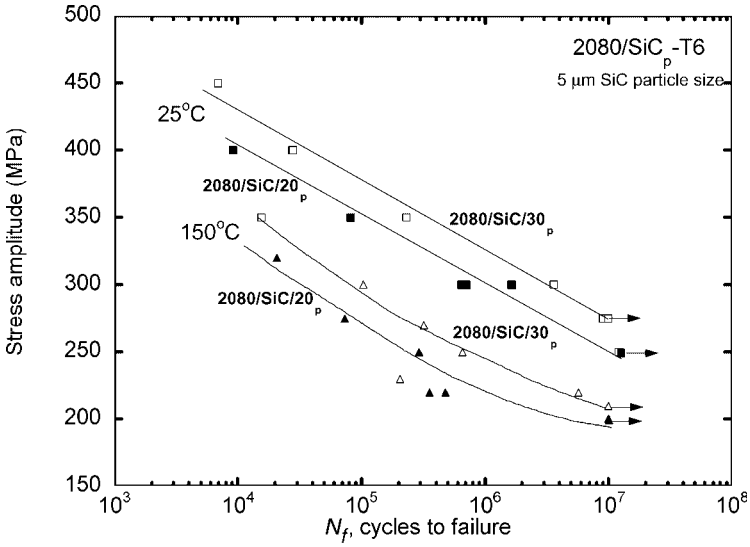

Fig. 22. Elevated temperature fatigue behavior of a patricle reinforced MMC. With increasing temperature, the matrix strength decreases resulting in decreased fatigue resistance (aging temperature was 175°C) (from Ref. 44).

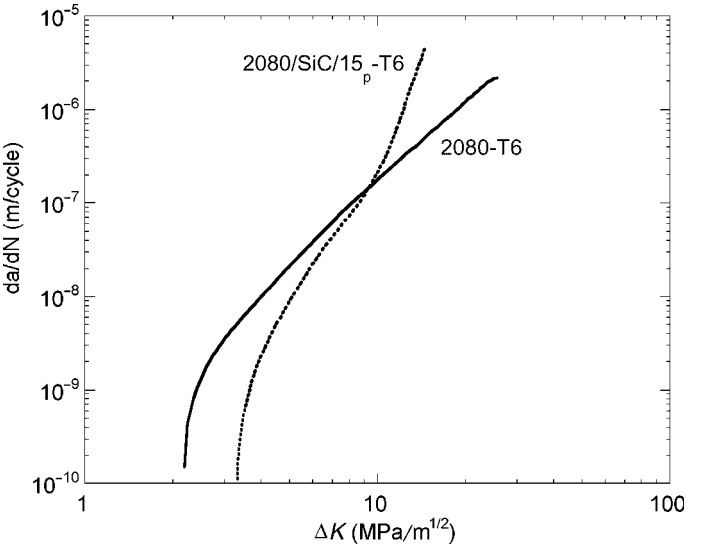

Fig. 23. Crack growth vs cyclic intensity factor for a particulate MMC versus the unreinforced alloy (after Ref. 46).

the material and test conditions (45):

$$da/dN = A\Delta\ K^m$$

The applied cyclic stress intensity range is given by

$$\Delta K = Y\Delta\sigma a^{1/2}$$

where Y is a geometric factor, $\Delta\sigma$ is the cyclic stress range, and a is the crack length. The principal concern in this kind of test is to make sure that there is only one dominant crack that is propagating. This is particularly a problem in fibrous composites. In the case of a particulate composite, frequently a dominant crack can be made to propagate and the above relationships can be used. A comparison of crack growth vs cyclic intensity factor for a particulate MMC and the unreinforced alloy is shown in Figure 23 (46). Higher threshold vales, ΔK_{th}, are observed for composites than for monolithic materials (47,48). The slope of da/dN vs ΔK in region II for the composites is generally comparable to the unreinforced alloys. Figure 24 shows some reinforcement and crack tip interactions in a particulate composite. At higher ΔK, the plastic zone around the crack tip is much larger than the particle size, and particle cracking takes place ahead of the crack tip. This results in planar crack growth. At lower ΔK, the plastic zone is much smaller so the crack avoids the SiC particles and grows in a tortuous fashion. Experimental evidence for this is shown in Figure 25. It appears that choosing the optimum particle size and volume fractions together with a clean matrix alloy results in a composite with improved fatigue characteristics.

Stiffness Loss in Fatigue. The complexities in composites lead to the presence of many modes of damage, such as matrix cracking, fiber fracture,

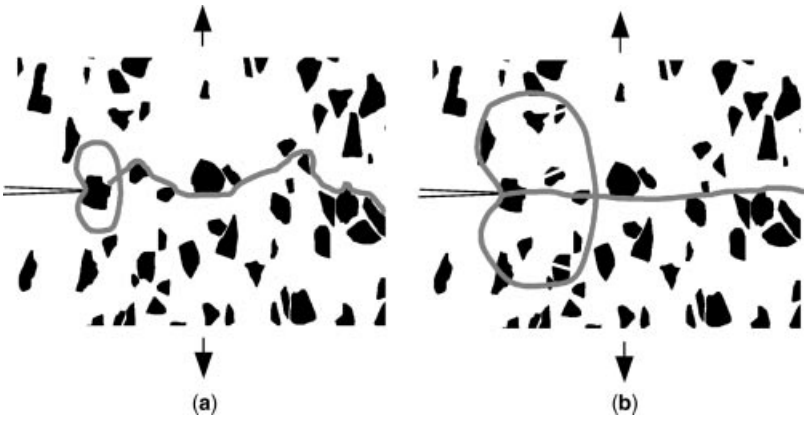

Fig. 24. Reinforcement and crack tip interactions in a particulate composite: (**a**) low K_{max}, ΔK, smaller plastic zone—tortuous crack growth takes place (**b**) high K_{max}, ΔK, larger plastic zone envelops several particles—particle fracture takes place ahead of the crack tip, resulting in planar crack growth.

delamination, debonding, void growth, multidirectional cracking, etc. In the case of the isotropic material, a single crack propagates in a direction perpendicular to the cyclic (mode I) loading axis (Fig. 26). In the fiber-reinforced composite, on the other hand, a variety of subcritical damage mechanisms (Fig. 27) lead to a highly diffuse damage zone, and these multiple fracture modes appear rather early in the fatigue life of composites. The various types of subcritical damage result in a reduction of the load carrying capacity of the laminate composite, which in turn manifests itself as a reduction of laminate stiffness and strength (49–53). The stiffness changes in the laminated composites to the accumulated damage under fatigue have been experimentally related. The change in stiffness values is a good indicator of the damage in composites, thus stiffness loss in continuous fiber-reinforced MMCs can be a useful parameter for detecting fatigue damage initiation and growth. This progressive loss of stiffness during fatigue of composites is a characteristic that is very different from the behavior of metals in fatigue. Similar loss of stiffness has been observed on subjecting a fiber-reinforced composite to thermal fatigue (54).

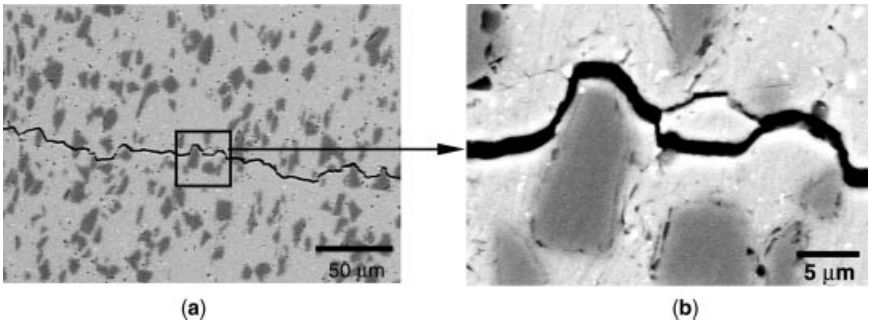

Fig. 25. Fatigue crack growth profile in a SiC particle reinforced Al matrix composite, exhibiting crack trapping and crack deflection mechanisms.

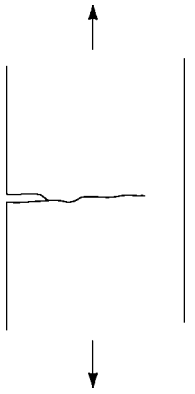

Fig. 26. Self-similar crack propagation in an isotropic material. The crack propagates in a direction perpendicular to the cyclic loading axis (mode I loading).

5.7. Creep. The phenomenon of creep refers to time-dependent deformation. In practice, at least for most metals and ceramics, the creep behavior becomes important at high temperatures and thus sets a limit on the maximum application temperature. In general, this limit increases with the melting point of a material. An approximate limit can be estimated to lie at about one-half of the melting temperature in kelvin. The basic governing equation of steady-state creep can be written as follows:

$$\dot{\epsilon} = A(\sigma/G)^n \exp(-\Delta Q/kT)$$

where $\dot{\epsilon}$ is the steady-state creep strain rate, σ is the applied strain, n is an exponent, G is the shear modulus, ΔQ is the activation energy for creep, k is the Boltzmann's constant, and T is temperature in kelvin. In general, the creep resistance of metal is improved by the incorporation of ceramic reinforcements. The steady-state creep rate as a function of applied stress for silver matrix and tungsten fiber–silver matrix composites at 600°C is an example (Fig. 28) (55). Whisker or particle reinforcement also results in significant

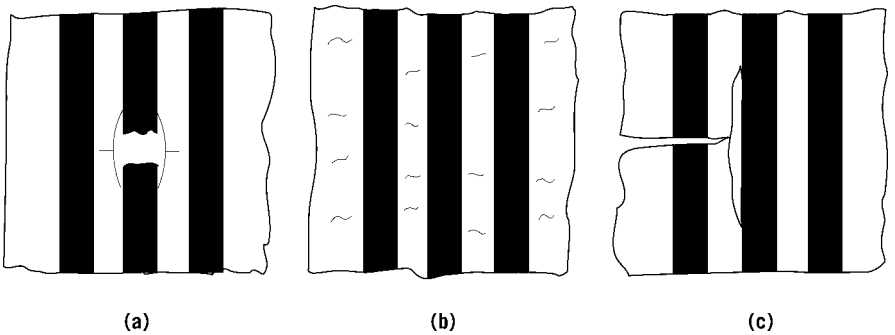

Fig. 27. Variety of subcritical damage mechanisms in fiber-reinforced composites, that lead to a highly diffuse damage zone. (**a**) Fiber cracking, (**b**) matrix cracking, and (**c**) interface debonding.

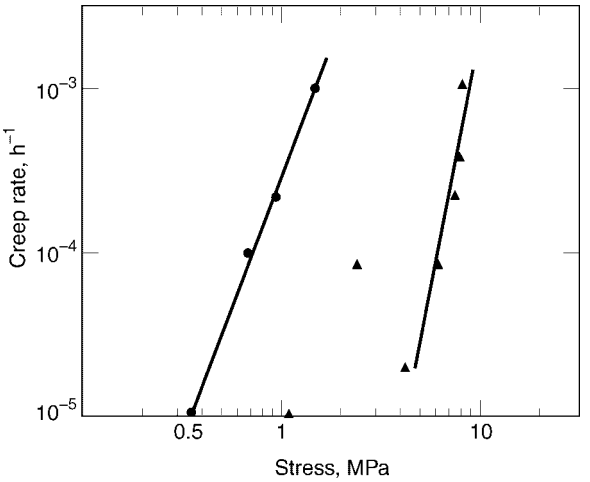

Fig. 28. Steady-state creep rate as a function of applied stress for silver matrix (•) and tungsten fiber–silver matrix composites (▲) at 600°C (from Ref. 55). To convert MPa to psi, multiply by 145.

creep strengthening over the unreinforced alloy, Figure 29 (56). Anomalously high values of the activation energy, Q, and stress exponent, n, have been reported in MMCs (57–59). Nardone and Strife (57) rationalized this by proposing the concept of a threshold stress σ_r, for creep deformation, originally used to explain the high values for Q and n in dispersion-strengthened alloys. The physical explanation for the threshold stress in the discontinuously reinforced

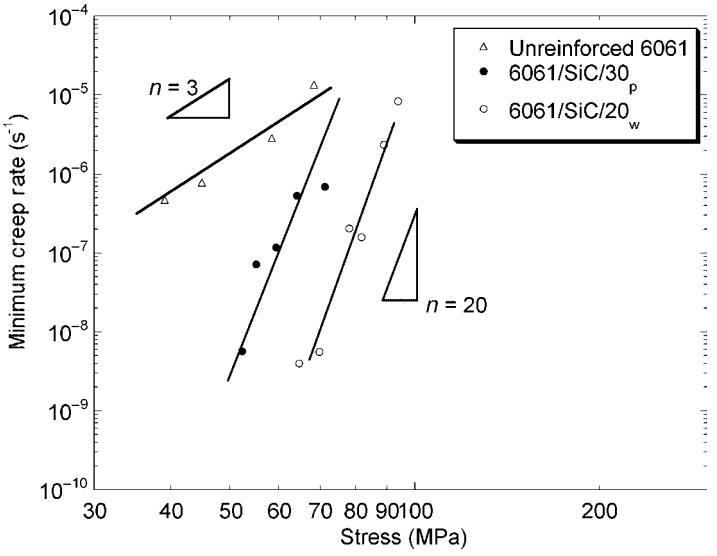

Fig. 29. Steady-state creep rate as a function of applied stress for SiC particle and SiC whisker reinforced Al matrix composites. To convert MPa to psi, multiply by 145 (from Ref. 56).

composite system can be attributed to a variety of reasons (58): (*1*) Orowan bowing between particles, (*2*) back-stress associated with dislocation climb, (*3*) attractive force between dislocations and particles, resulting from relaxation of the strain field of dislocations at the particle–matrix interface.

6. Applications

In aerospace applications, low density coupled with other desirable features, such as tailored thermal expansion and conductivity, high stiffness and strength, etc, are the main drivers. Performance rather than cost is the driving force for materials development. In as much as continuous fiber-reinforced MMCs deliver superior performance to particle-reinforced composites, the former are frequently used in aerospace applications. In nonaerospace applications, cost and performance are important, ie, an optimum combination of these items is required. It is thus understandable that particle-reinforced MMCs are increasingly finding applications in nonaerospace applications.

Reduction in the weight of a component is a significant driving force for any application in the aerospace field. For example, in the Hubble telescope, a pitch-based continuous carbon fiber-reinforced aluminum was used for waveguide booms because of its light weight; high elastic modulus, E; and low coefficient of thermal expansion, α. Other aerospace applications of MMCs involve replacement of light but toxic beryllium. For example, in the United States Trident missile, beryllium has been replaced by a SiC_p/Al composite.

An important application of MMCs in the automotive area is in diesel piston crowns (57). This application involves incorporation of short fibers of alumina or alumina–silica in the crown of the piston. The conventional diesel engine piston has an Al-Si casting alloy with a crown made of a nickel cast iron. The replacement of the nickel cast iron by aluminum matrix composite results in a lighter, more abrasion resistant, and cheaper product. Another application in the automotive sector involves the use of carbon and alumina short fibers in an aluminum matrix for use as cylinder liners in the Prelude model of Honda Motor Co.

Particulate MMCs, especially with light MMCs such as aluminum and magnesium, also find applications in automotive and sporting goods. In this regard, the price per kg becomes the driving force for application. An excellent example involves the use of Duralcan particulate MMCs to make mountain bicycles. The Specialized Bicycle company in the Unites States sells these bicycles with the frame made from extruded tubes of 6061 aluminum containing about 10% alumina particles. The primary advantage is the gain in stiffness. An important item in this regard has to do with recycling and reclamation, particularly in aluminum matrix composites, because recycling has been extremely successful in the aluminum industry. The two terms, recycling and reclamation, are used advisedly for composites. Recycling (qv) refers to reuse of a worn product as a composite, and involves reclamation of the individual components, ie, aluminum and ceramic particles separately. Cast MMCs can be remelted and reused as a composite. Although some of the issues such as particle/molten metal reaction are the same in remelting, it should be appreciated that scrap sorting and

melt cleanliness and degassing can be rather complex problems in MMCs. Special fluxing and degassing techniques have been developed at Duralcan. Powder processed MMCs as well as the reclamation route involve remelting. According to one report (58), by using combined argon and salt fluxing, silicon carbide particles can be removed from the melt and 85–90% of the aluminum reclaimed.

An important potential commercial application of particle-reinforced aluminum composite is in the making of automotive driveshafts. In driveshaft design, the speed at which it becomes dynamically unstable needs to be considered. In terms of geometric parameters, a shorter shaft length and larger diameter gives a higher critical speed, N_c; in terms of material parameters, the higher the specific stiffness E/r, the higher the N_c. Changes in the driveshaft geometry, increase in length or a reduction in the diameter, can be made while maintaining a constant critical speed. A decrease in the driveshaft diameter can be important because of under-chassis space limitations. A relatively new application for MMCs is the passenger car connecting rod. Recently, lightweight MMC connecting rods were fabricated using a low cost sinter-forging technique. Figure 30 shows a 3D model of the MMC connecting rod, which exhibited close to 60% weight savings over the conventional steel connecting rod.

Copper-based composites having Nb, Ta, or Cr as the second phase in a discontinuous form are of interest for certain applications requiring high thermal conductivity and high strength, eg, in high heat flux applications in rocket engine thrust chambers. Carbon fiber-reinforced copper has applications in the aerospace industry as a very high thermal conductivity material. The problem with carbon fibers and metallic matrices is that the surface energy considerations preclude wetting of the carbon fibers by the molten metals. The surface energy of carbon fiber is $\sim$100 mJ/m^2, whereas for most molten metals the surface energy is 10 times higher. Wetting occurs when the surface energy of the substrate (fiber) is higher than that of the molten metal. Thus the wetting of carbon fibers by molten copper is not expected.

6.1. Filamentary Superconductors. Niobium–titanium superconductors are used in magnetic resonance imaging (MRI) techniques for medical diagnostics. The superconducting solenoid made from Nb-Ti/Cu composite wire is immersed in a liquid helium cryogenic Dewar flask. Nb-Ti/Cu superconducting

	ALMMC	Steel
Pin Weight (g)	65.2	144.7
Crank Weight (g)	184.0	437.7
Total Weight (g)	249.2	582.4

Weight savings = 57.2%

Fig. 30. Prototype MMC connecting rod fabricated by sinter-forging. The 20% SiC reinforced Al matrix composite exhibited close ot 60% weight savings over the conventional steel rod (courtesy Metaldyne Corp.).

composites are also used in various high energy physics applications, such as particle accelerators. The Nb_3Sn/Cu superconducting composites are used for magnetic fields >12 T. Such high fields are encountered in a thermonuclear fusion reactor, representing a sizeable fraction of the capital cost of such a fusion power plant.

6.2. Electronic-Grade MMCs. Metal-matrix composites can be tailored to have optimal thermal and physical properties to meet requirements of electronic packaging systems, eg, cores, substrates, carriers, and housings. A controlled thermal expansion space truss, ie, one having a high precision dimensional tolerance in space environment, was developed from a carbon fiber (pitch-based)/Al composite. Continuous boron fiber-reinforced aluminum composites made by diffusion bonding have been used as heat sinks in chip carrier multilayer boards.

Unidirectionally aligned, pitch-based carbon fibers in an aluminum matrix can have high thermal conductivity along the fiber direction. The conductivity transverse to the fibers is about two-thirds that of aluminum. Such a C/Al composite is useful in heat-transfer applications where weight reduction is an important consideration, eg, in high density, high speed integrated circuit packages for computers and in base plates for electronic equipment. Another possible use of this composite is to dissipate heat from the leading edges of wings in high speed airplanes.

BIBLIOGRAPHY

"Laminated and Reinforced Metals" in *ECT* 3rd ed., Vol. 13, pp. 941–967, by C. C. Chamis, National Aeronautics and Space Administration; "Metal-Matrix Composites" in *ECT* 4th ed., Vol. 16, pp. 392–415, by K. K. Chawla, New Mexico Institute of Mining and Technology; "Metal-Matrix Composites" in *ECT* (online), posting date: December 4, 2000, by K. K. Chawla, New Mexico Institute of Mining and Technology.

CITED PUBLICATIONS

1. K. K. Chawla, *Composite Materials: Science and Engineering*, 2nd ed., Springer-Verlag, New York, 1999.
2. C. R. Kennedy, in P. Vincenzine, ed., *Proceedings of the 7th CIMTEC-World Ceramics Congress*, Elsevier, New York, 1991, p. 691.
3. A. J. Cook and P. S. Warner, *Mater. Sci. Eng.* **A144**, 189 (1991).
4. R. Saha, E. Morris, N. Chawla, and S. M. Pickard, *J. Mater. Sci. Lett.* **21**, 337 (2002).
5. S. Nourbakhsh, F. L. Liang, and H. Margolin, *Met. Trans. A* **21A**, 213 (1990).
6. K. K. Chawla and L. B. Godefroid, *Proceedings of the 6th International Conference on Fracture*, Pergamon Press, Oxford, U.K., 1984, p. 2873.
7. W. H. Hunt, T. M. Osman, and J. J. Lewandowski, *J. Miner. Metal Mater. Soc.* 30 (Mar. 1991).
8. M. Manoharan, L. Ellis, and J. J. Lewandowski, *Scr. Met. Mater.* **24**, 1515 (1990).
9. K. H. Sandhage, G. N. Riley, Jr., and W. L. Carter, *J. Miner. Metal. Mater. Soc.* (Mar. 1991).

10. W. H. Hunt, in *Processing and Fabrication of Advanced Materials*, The Minerals, Metals and Materials Society, Warrendale, Pa., 1994, pp. 663–683.
11. V. V. Ganesh and N. Chawla, and J. R. Michael, unpublished work.
12. N. Chawla, J. J. Williams, and R. Saha, *J. Light Metals* **2**, 215 (2002).
13. X. Deng, C. Cleveland, and N. Chawla, unpublished work.
14. E. J. Lavernia, E. Gutierrez, and J. Baram, *Mater. Sci. Eng.* **132A**, 119 (1991).
15. R. Mitra, W. A. Chiou, M. E. Fine, and J. R. Weertman, *J. Mater. Res.* **8**, 2300 (1993).
16. R. G. Hill, R. P. Nelson, and C. L. Hellerich, *Proceedings of the 16th Refractory Working Group Meeting*, Seattle, Wash., Oct. 1969.
17. K. K. Chawla and M. Metzger, *Advances in Research on Strength and Fracture of Materials*, Vol. 3, Pergamon Press, New York, 1978, p. 1039.
18. A. R. Champion, W. H. Krueger, H. S. Hartman, and A. K. Dhingra, *Proceedings of the 2nd International Conference on Composite Materials (ICCM/2)*, TMS-AIME, New York, 1978, p. 883.
19. V. V. Ganesh and N. Chawla, *Metall. Mater. Trans.* **35A**, 53–62 (2004).
20. K. K. Chawla and M. Metzger, *J. Mater. Sci.* **7**, 34 (1972).
21. K. K. Chawla, *Metallography* **6**, 155 (1973).
22. K. K. Chawla, *Philos. Mag.* **28**, 401 (1973).
23. K. K. Chawla, *Fibre Sci. Tech.* **8**, 49 (1975).
24. N. S. Stoloff, *Advances in Composite Materials*, Applied Science Publishers, London, p. 247.
25. D. L. McDanels and R. A. Signorelli, *NASA TN D*, 8204 (1976).
26. A. P. Majidi and T. W. Chou, *Proc. ICCM VI* **2**, 422 (1987).
27. D. F. Hasson and C. R. Crowe, *Strength of Metals and Alloys*, Pergamon Press, Oxford, U.K., 1985, pp. 1515–1520.
28. N. Chawla, B. V. Patel, M. Koopman, K. K. Chawla, R. Saha, B. R. Patterson, E. R. Fuller, and S. A. Langer, *Mater. Charac.* **49**, 395 (2003).
29. R. J. Arsenault and R. M. Fisher, *Scripta Met.* **17**, 67 (1983).
30. E. H. Kerner, *Proc. Phys. Soc.* **69**, 808 (1956).
31. P. S. Turner, *J. Res. NBS* **37**, 239 (1946).
32. R. A. Schapery, *J. Comp. Mater.* **2**, 311 (1969).
33. R. U. Vaidya and K. K. Chawla, in K. Upadhya, ed., *Developments in Metal and Ceramic Matrix Composites*, The Minerals, Metals and Materials Society, Warrendale, Pa., 1991, pp. 253–272.
34. H. J. Rack, *The Sixth International Conference on Composite Materials*, Elsevier Applied Science Publishers, New York, 1987, p. 382.
35. T. Christman and S. Suresh, *Mater. Sci. Eng.* **102A**, 211 (1988).
36. K. K. Chawla, A. H. Esmaeili, A. K. Datye, and A. K. Vasudevan, *Scripta Met. Mater.* **25**, 1315 (1991).
37. S. Suresh and K. K. Chawla, in S. Suresh, A. Needleman, and A. Mortensen, eds., *Metal Matrix Composites*, Butterworth-Heinemann, Boston, Mass., 1993.
38. N. Chawla, L. C. Davis, C. Andres, J. E. Allison, J. W. Jones, *Metall. Mater. Trans. A.* **31A**, 951 (2000).
39. N. Chawla, U. Habel, Y.-L. Shen, C. Andres, J. W. Jones, and J. E. Allison, *Metall. Mater. Trans. A.* **31A**, 531 (2000).
40. D. R. Williams and M. E. Fine, *Proceedings of the 5th International Conference on Composite Materials (ICCM/V)*, TMS-AIME, Warrendale, Pa., 1985, p. 639.
41. M. A. McGuire and B. Harris, *J. Phys. D: Appl. Phys.* **7**, 1788 (1974).
42. N. Chawla, C. Andres, J. W. Jones, and J. E. Allison, *Metall. Mater. Trans. A.* **29A**, 2843 (1998).

43. J. J. Bonnen, C. P. You, J. E. Allison, and J. W. Jones, in *Proceedings of the International Conference on Fatigue*, Pergamon Press, New York, 1990, pp. 887–892.
44. N. Chawla, J. W. Jones, and J. E. Allison, in X. R. Wu and Z. G. Wang, eds., *Fatigue '99*, EMAS/HEP, 1999.
45. P. C. Paris and F. Erdogan, *J. Basic Eng. Trans. ASME* **85**, 528 (1963).
46. D. A. Lukasak and R. J. Bucci, Alloy Technology Division, Report. No. KF-34, Alcoa Technical Center, Alcoa Center, Pa., 1992.
47. J. K. Shang, W. Yu, and R. O. Ritchie, *Mater. Sci. Eng.* **A102**, 181 (1988).
48. D. L. Davidson, *Eng. Fract. Mech.* **33**, 965 (1989).
49. H. T. Hahn and R. Y. Kim, *J. Comp. Mater.* **10**, 156 (1976).
50. A. T. Highsmith and K. L. Reifsnider, *Damage in Composite Materials*, ASTM STP 775, ASTM, Philadelphia, Pa., 1982, p. 103.
51. R. Talreja, *Fatigue of Composite Materials*, Technical University of Denmark, Lyngby, 1985.
52. T. K. O'Brien and K. L. Reifsnider, *J. Comp. Mater.* **15**, 55 (1981).
53. S. L. Ogin, P. A. Smith, and P. W. R. Beaumont, *Composites Sci. Tech.* **22**, 23 (1985).
54. Z. R. Xu, K. K. Chawla, A. Wolfenden, A. Neuman, G. M. Liggett, and N. Chawla, *Mater. Sci. Eng. A* **A203**, 75 (1995).
55. A. Kelly and W. R. Tyson, *J. Mech. Phys. Solids* **14**, 177 (1966).
56. D. Webster, *Metall. Mater. Trans.* **13A**, 1511 (1982).
57. V. C. Nardone and J. R. Strife, *Metall. Trans.* **18A**, 109 (1987).
58. D. C. Dunand and B. Derby, *Fundamentals of Metal Matrix Composites*, Butterworth-Heinneman, Boston, 1993, pp. 191–214.
59. Y. Li and T. G. Langdon, *Mater. Sci. Eng.* **A265**, 276 (1999).
60. T. Donomoto, N. Miura, K. Funatani, and N. Miyake, *SAE Technical Paper*, No. 83052, Detroit, Mich., 1983.
61. D. J. Lloyd, *Int. Mater. Rev.* **39**, 1 (1994).

GENERAL REFERENCES

A. Evans, C. S. Marchi, and A. Mortensen, *Metal Matrix Composites in Industry*, Kluwer Academic Pub., Dordrecht, 2003.
K. K. Chawla, *Composite Materials: Science and Engineering*, 2nd ed., Springer-Verlag, New York, 1998.
N. Chawla and K. K. Chawla, *Metal Matrix Composites*, Kluwer Academic Publishers, Boston, 2004, in preparation.
N. Chawla and Y.-L. Shen, *Adv. Eng. Mater.* **3**, 357 (2001).
S. Suresh, A. Needleman, and A. Mortensen, eds., *Metal Matrix Composites*, Butterworth-Heinemann, Boston, Mass., 1993.

KRISHAN K. CHAWLA
University of Alabama at Birmingham
N. CHAWLA
Arizona State University